535

SIMULATION OF SEMICONDUCTOR DEVICES AND PROCESSES Vol. 4
Edited by W. Fichtner, D. Aemmer - Zurich (Switzerland) September 12-14, 1991 - Hartung-Gorre

Self Adaptive Computation of the Breakdown Voltage of Planar pn-Junctions with Multistep Field Plates

Ralf Kornhuber and Rainer Roitzsch

Konrad-Zuse-Zentrum (ZIB), W-1000 Berlin 31, Fed. Rep. Germany

Abstract

The breakdown voltage highly depends on the electric field in the depletion area whose computation is the most time consuming part of the simulation. We present a self adaptive Finite Element Method which reduces dramatically the required computation time compared to usual Finite Difference Methods. A numerical example illustrates the efficiency and reliability of the algorithm.

It is a well accepted criterion for the breakdown of pn-junctions that the ionization integrals

$$
\begin{aligned}
I_n &= \int_0^w \alpha_n \exp(-\int_\xi^w (\alpha_n - \alpha_p) d\eta) d\xi \\
I_p &= \int_0^w \alpha_p \exp(-\int_0^\xi (\alpha_p - \alpha_n) d\eta) d\xi
\end{aligned}
\tag{1}
$$

for electrons and holes reach the value one

$$
I_n = 1 , \quad I_p = 1 . \tag{2}
$$

As impact ionization is likely to happen in regions of large field strength, the condition (2) is tested only for field lines crossing the relative maxima of $|E|$ (see [1] for details).

As the ionization rates α_n, α_p depend on E according to the law of Chynoweth [2]

$$
\alpha_i = \alpha_i \exp(-(b_i/|E|)^{m_i}) , \quad i = n, p , \tag{3}
$$

with parameters α_i, b_i, m_i, $i = n, p$, given in [3], the crucial part of the evaluation of I_n, I_p is the computation of the electric field. In the case of strongly reverse biased pn-junctions which are considered here the full depletion assumption

$$
n = qD\delta_{\psi,0} , \quad p = -qD\delta_{\psi,-\psi_0} \tag{4}
$$

is justified. Here $\delta_{x,y}$ is defined by $\delta_{x,y} = 1$ if $x = y$ and $\delta_{x,y} = 0$ if $x \neq y$ (Kronecker symbol), ψ denotes the potential distribution, D the doping concentration and $-\psi_0$, 0 are the voltages applied to the anode and cathode respectively. Substituting (4) in the well-known drift-diffusion equations [4] we are left with the single nonlinear equation [5]

$$
- \operatorname{div}(\varepsilon \nabla \psi) = qD(1 - \delta_{\psi,0} - \delta_{\psi,-\psi_0}) \tag{5}
$$

on the computational domain Ω together with transition and boundary conditions. It is well-known (see Hunt/Nassif [6]) that a weak solution of (5) is obtained as the minimum of the energy functional

$$
F(\varphi) = \tfrac{1}{2} a(\varphi, \varphi) - l(\varphi) \tag{6}
$$

with $a(\cdot,\cdot)$ and $l(\cdot)$ given by

$$\begin{aligned} a(\varphi_1,\varphi_2) &= \int_\Omega \varepsilon \nabla\varphi_1 \cdot \nabla\varphi_2 \, d(x,y) \,, \\ l(\varphi) &= q \int_\Omega D\varphi \, d(x,y) \,, \end{aligned} \tag{7}$$

on the convex set K,

$$K = \{\varphi \in H \mid -\psi_0 \le \varphi \le 0 \text{ almost everywhere on } \Omega\} \tag{8}$$

where H consists of all functions φ with finite energy

$$\|\varphi\| := a(\varphi,\varphi)^{\frac{1}{2}} < \infty \,, \tag{9}$$

satisfying the Dirichlet boundary conditions. Hence we mainly concentrate on the self adaptive Finite Element approximation of the minimization problem:

$$\text{Find } \psi \in K \text{ such that } F(\psi) \le F(\varphi) \,, \quad \varphi \in K \,. \tag{10}$$

Once an approximate solution Ψ is computed the ionization integrals I_n, I_p are evaluated as described in Section 5.

1 Self Adaptive Finite Element Discretization

Let $\mathcal{T}$ denote a triangulation of $\Omega \subset \mathrm{I\!R}^2$ with vertices $\mathcal{P}$ and edges $\mathcal{E}$ respectively. Using the standard basis functions λ_p, $p \in \mathcal{P}$ with the property $\lambda_p(q) = \delta_{p,q}$ the desired Finite Element approximation Ψ is written as

$$\Psi = \Psi^C + \sum_{p \in \mathcal{P}^0} \Psi_p \lambda_p \tag{11}$$

with Ψ^C representing the Dirichlet boundary conditions and $\mathcal{P}^0 \subset \mathcal{P}$ denoting the remaining vertices on which the value Ψ_p of Ψ is unknown. Substituting (11) in (10) we obtain the Finite Element discretization

Find the vector $\underline{\Psi} = (\Psi_p)_{p\in\mathcal{P}^0} \in K^L$ with $K^L = \{\underline{\varphi} = (\varphi_p)_{p\in\mathcal{P}^0} \mid -\psi_0 \le \varphi_p \le 0\}$

such that $\underline{\Psi}^T(A\underline{\Psi} - b) = \min_{\underline{\varphi} \in K^L}$. $\tag{12}$

The stiffness matrix A and the right–hand side b have the entries

$$a_{pq} = \tfrac{1}{2} a(\lambda_q, \lambda_p) \,, \quad b_p = l(\lambda_p) - a(\Psi^C, \lambda_p) \,, \quad p, q \in \mathcal{P}^0 \,. \tag{13}$$

The important question how to chose the triangulation $\mathcal{T}$ is left open in classical Finite Element Methods. We propose a self adaptive method which is roughly described as follows:

Algorithm 1. Self Adaptive Finite Element Algorithm

Step 0: Start with an intentionally coarse triangulation $\mathcal{T}_0$ on level 0.

Step 1: Compute an iterate $\tilde{\Psi}_k$ sufficiently close to the Finite Element approximation Ψ_k with respect to the triangulation $\mathcal{T}_k$ on level $k \ge 0$.

Step 2: Compute a local estimate of the total error $\|\tilde{\Psi}_k - \psi\|$.

Step 3: If $\tilde{\Psi}_k$ is accurate enough, then stop. Else refine all edges on which the local errors are too large resulting in a finer triangulation $\mathcal{T}_{k+1}$ and go to Step 1.

This approach is widely used in self adaptive methods [7, 8]. For Step 0 we refer to [9]. The remaining steps are described in the subsequent sections.

2 Iterative Solution

A convergent sequence of iterate Ψ_k^ν, $\nu = 0, \ldots$, can be computed by well-known relaxation methods as described for instance in [10]. See also [1, 11, 12]. Assuming that the discretization error behaves like

$$\|\Psi_k - \psi\| \leq c N_k^{-\frac{1}{2}}, \quad k = 0, 1, \ldots \tag{14}$$

with $N_k = |\mathcal{P}_k^0|$ denoting the number of unknowns, the iteration should be stopped if

$$\|\Psi_k^\nu - \psi\| \leq \tilde{c} N_k^{-\frac{1}{2}}, \quad \tilde{c} \approx c. \tag{15}$$

It can be shown along the lines of [8] that (15) holds with $\tilde{c} \leq 3c$ provided that

$$\|\Psi_0^\nu - \Psi_0\| \leq \tfrac{1}{2} \|\Psi_0^\nu - \psi\|, \quad k = 0, \tag{16}$$

$$\|\Psi_k^\nu - \Psi_k\| \leq \tfrac{1}{2} \varrho_{k-1} \|\tilde{\Psi}_{k-1} - \psi\|, \quad k > 0, \tag{17}$$

with $\varrho_{k-1} = (N_{k-1}/N_k)^{1/2}$, $k > 0$. Hence (16) and (17) are used as stopping criterion for the iterative solution. We write $\tilde{\Psi}_k := \Psi_k^\nu$ as soon as (16), (17) are fulfilled. Note that for $k > 0$ the total error appearing on the right-hand side of (17) is available from Step 2 of Algorithm 1 on level $k - 1$. To estimate the iteration error $\delta_k^\nu = \|\Psi_k^\nu - \Psi_k\|$ we use the well-known error estimate for fixed point iterations. Here the contraction number is replaced by the quotient of subsequent iterates. The iterative solution can be accelerated by multi level methods as proposed in [13]. These concepts will enter future revisions of the program.

3 Local Error Estimation

To obtain an estimate $\tilde{\varepsilon}_k$ of the total error $\varepsilon_k = \|\tilde{\Psi}_k - \psi\|$ we proceed in two main steps.

- Replace the exact solution ψ by the piecewise quadratic approximation Φ_k.

- Localize the computation of Φ_k by suitable simplifications.

Along the lines of Section 1 we use the representation

$$\Phi_k = \Psi_k^C + \Psi_k^L + \Psi_k^Q \tag{18}$$

with Ψ_k^C taken from (11) and

$$\Psi_k^L = \sum_{p \in \mathcal{P}_k^0} \Psi_p^L \lambda_p, \quad \Psi_k^Q = \sum_{e \in \mathcal{E}_k^0} \Psi_e^Q \mu_e \tag{19}$$

where $\mathcal{E}_k^0 \subset \mathcal{E}_k$ contains all edges which are not part of the Dirichlet boundary and μ_e is piecewise quadratic satisfying $\mu_e(q) = \delta_{pq}$ for $p = $ midpoint of e and $q \in \mathcal{P}_k^0 \bigcup \{$midpoints of edges in $\mathcal{E}_k^0\}$. Substituting (18) in (10) we obtain the following discretization of higher order.

Find $\underline{\Psi}^L = (\Psi_p^L)_{p \in \mathcal{P}_k^0}$ and $\underline{\Psi}^Q = (\Psi_e^Q)_{e \in \mathcal{E}_k^0}$ with $(\underline{\Psi}^L, \underline{\Psi}^Q) \in K^{L,Q}$ and

$$K^{L,Q} = \{(\underline{\varphi}^L, \underline{\varphi}^Q)| -\psi_0 \leq \varphi_p^L \leq 0, \ p \in \mathcal{P}_k^0, \\ -\psi_0 \leq \varphi_e^Q + (\varphi_{p_1}^L + \varphi_{p_2}^L)/2 \leq 0, e = (p_1, p_2) \in \mathcal{E}_k^0\} \tag{20}$$

such that $\left(\begin{array}{c}\psi_k^L \\ \psi_k^Q\end{array}\right)^T \left[\left(\begin{array}{cc}A_{LL} & A_{LQ} \\ A_{QL} & A_{QQ}\end{array}\right)\left(\begin{array}{c}\underline{\Psi}_k^L \\ \underline{\Psi}_k^Q\end{array}\right) - \left(\begin{array}{c}b^L \\ b^Q\end{array}\right)\right] = \min_{(\varphi^L, \varphi^Q) \in K^{L,Q}}$.

Note that the splitting (18) results in a corresponding block structure of the stiffness matrix. Of course (20) has to be simplified for complexity reasons. This is done in two steps.

- Replace the quadratic part A_{QQ} by its diagonal D_{QQ}.

- Apply one step of a Block–Jacobi Method to the start iterate $(\underline{\tilde{\Psi}}_k, 0)$.

In this way our initial problem (12) is recovered for the approximate linear part $\underline{\tilde{\Psi}}_k^L$. Note that (12) is already solved up to an approximate iteration error. For the quadratic part we obtain the problem:

Find $\underline{\tilde{\Psi}}_k^Q = (\tilde{\Psi}_e^Q)_{e \in \mathcal{E}_k^0}$ with $(\underline{\tilde{\Psi}}_k, \underline{\tilde{\Psi}}_k^Q) \in K^{L,Q}$

$$\text{such that } (\underline{\tilde{\Psi}}_k^Q)^T \left[D_{QQ}\underline{\tilde{\Psi}}_k^Q - (b^Q - 2A_{QL}\underline{\tilde{\Psi}}_k)\right] = \min_{(\Psi_k, \varphi^Q) \in K^{L,Q}} . \tag{21}$$

Obviously (21) reduces to a one dimensional obstacle problem for each edge $e \in \mathcal{E}_k^0$ which is easily solved exactly. Using the energy norm $|\varphi|_M = (\varphi^T, M\varphi)^{1/2}$ we obtain the total error estimate

$$(\tilde{\varepsilon}_k) = \left(|\underline{\tilde{\Psi}}_k - \underline{\tilde{\Psi}}_k|_{A_{LL}}^2 + |\underline{\tilde{\Psi}}_k^Q|_{D_{LL}}^2\right)^{\frac{1}{2}} . \tag{22}$$

4 Refinement Techniques

The refinement is based on the local errors

$$\eta(e) = a_{ee}(\tilde{\Psi}_e^Q)^2 , \quad e \in \mathcal{E}_k^0 , \tag{23}$$

with a_{ee} denoting the appropriate diagonal element of A_{QQ} and $\underline{\tilde{\Psi}}_k^Q = (\tilde{\Psi}_e^Q)_{e \in \mathcal{E}_L^0}$ computed above.

Now the subset $\mathcal{E}_k' \subset \mathcal{E}_k$ which is marked for refinement consists of all edges e for which $\eta(e)$ is large, i.e.

$$\mathcal{E}_k' = \{e \in \mathcal{E}_k^0 | \eta(e) \geq \eta_k\} .$$

with some suitable threshold value η_k. For $k > 0$ a guess of the maximal error occurring on the next level in case of uniform refinement is used as threshold value. This guess is made by extrapolation as proposed in [14]. See [10] for details.

Let $\mathcal{T}_k' \subset \mathcal{T}_k$ denote the set of all triangles with at least one edge in $\mathcal{E}_k'$. Then each $t \in \mathcal{T}_k'$ is refined using either red or blue refinement as shown in Figures 1 and 2. Note that blue refinement is used to improve the angles of flat triangles which may be used for the efficient resolution of horizontal layer structures typically arising in semiconductor devices. We refer to [10] and [9] for details. After possible refinement of further triangles which may be necessary for structural reasons the process is stopped by green closures as shown in Figure 3.

5 Ionization Integrals

Once an approximation $\tilde{E}_k = -\nabla\tilde{\Psi}_k$ of the electric field is computed on level k, the evaluation of the ionization integrals I_n, I_p defined in (1) is performed as follows:
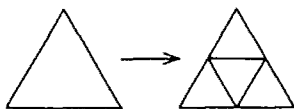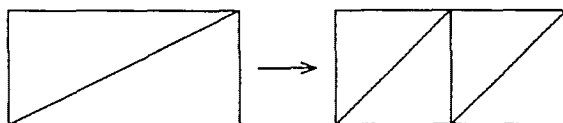
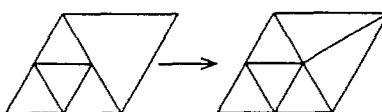Figure 1: Red refinement

Figure 2: Blue refinement

Figure 3: Green closure

Algorithm 2. Ionization Integrals

Step 1: Find the set $T_k^{\max} \subset T_k$ of triangles on which $|\tilde{E}_k|$ has a relative maximum.

Step 2: For each $t \in T_k^{\max}$ collect the field line γ_t intersecting t.

Step 3: For each γ_t, $t \in T_k^{\max}$ evaluate the corresponding integrals $\tilde{I}_n(\gamma_t)$, $\tilde{I}_p(\gamma_t)$. Select the maximal ionization integrals $\tilde{I}_p$, $\tilde{I}_n$ for all $t \in T_k^{\max}$.

Recall that $\tilde{E}_k$ is constant on each $t \in T_k$. Hence the evaluation of the ionization integrals with E replaced by $\tilde{E}_k$ can be performed exactly. Finally $\tilde{I}_n$, $\tilde{I}_p$ are used to check the criterion (2) for the breakdown of the considered device.

6 Numerical Results

The method is applied to a planar pn-junction with multistep field plate shown in Figure 4. Note that the representation is not in scale. We refer to [10] for the physical data.

Figure 6 shows an initial triangulation T_0 generated semi-automatically by the program BOXES [9] with the equipotential lines of the corresponding approximation Ψ_0 depicted in Figure 7. The Figures 8 and 9 show the final triangulation T_6 generated automatically from T_0 and the corresponding approximation Ψ_6 for the applied voltage $-\psi_0 = 800V$. In Figure 9 we have also depicted the boundary of the depletion area Ω_D together with the field line γ along which the maximal ionization integral $\tilde{I}_p$ is obtained. The dependence of $\tilde{I}_p$ on the applied voltage $-\psi_0$ is shown in Figure 5.
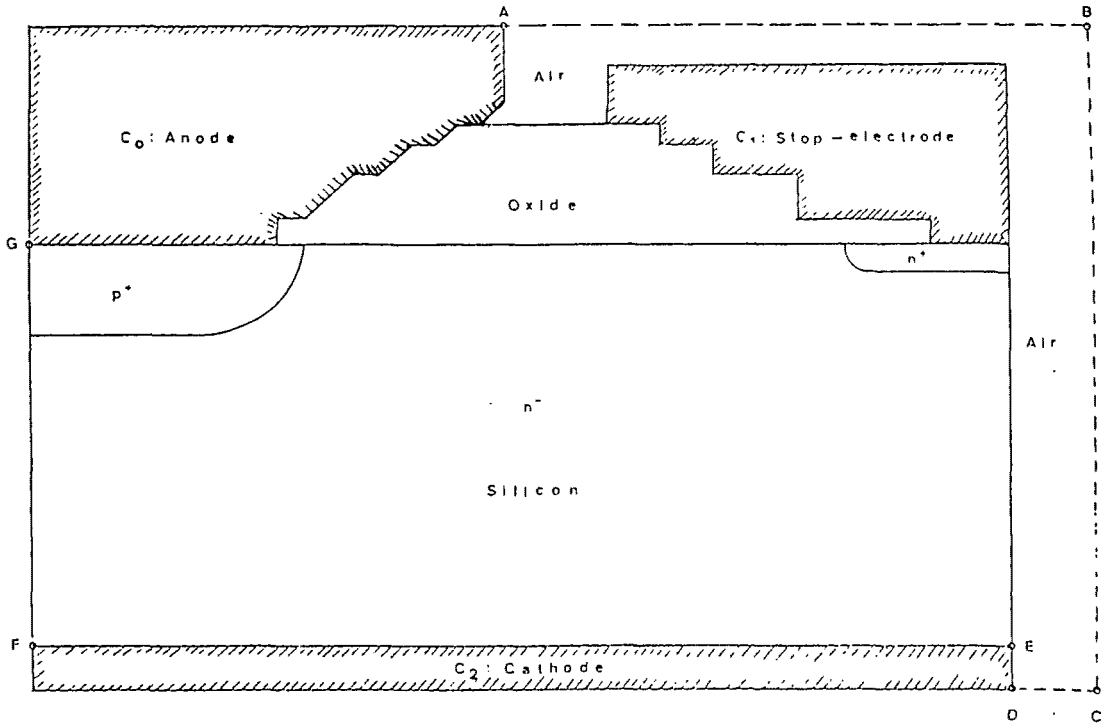
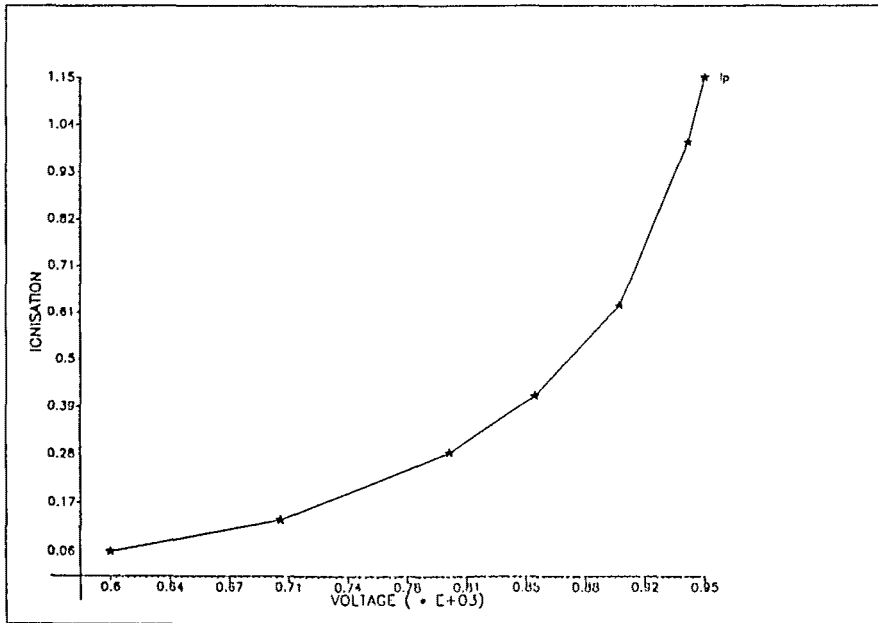Figure 4: Geometry of the computational domain

Figure 5: Dependence of the ionisation integral I_p on the applied voltage $-\psi_0$
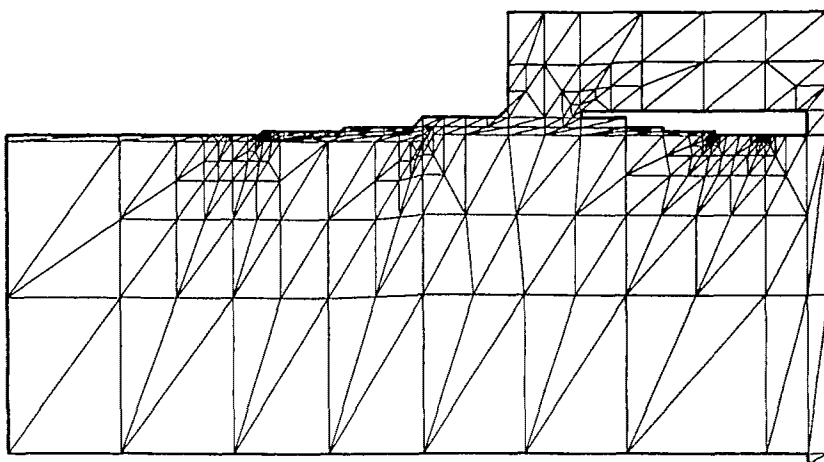
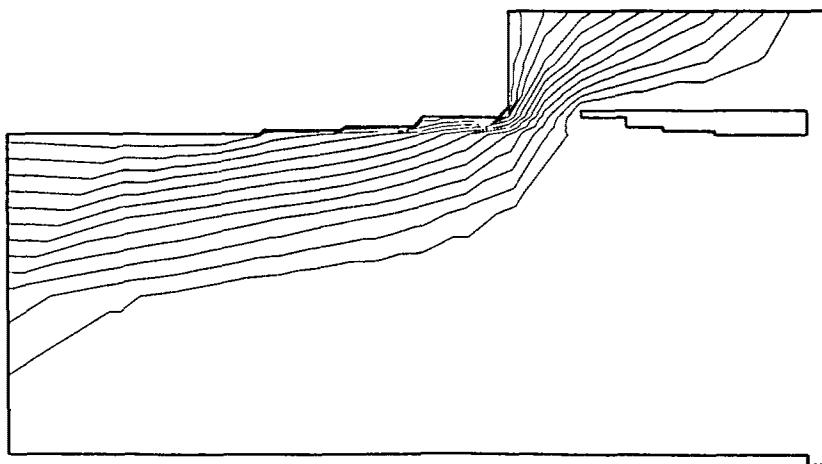Figure 6: Initial triangulation generated by BOXES (371 nodes)

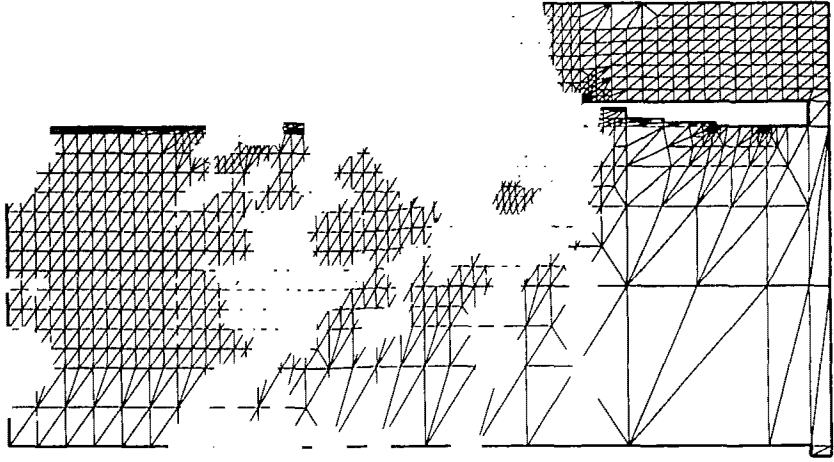Figure 7: Level curves of initial solution Ψ_0 corresponding to $\mathcal{T}_0$

Figure 8: Final triangulation $\mathcal{T}_6$ obtained by self–adaptive refinement (2042 nodes)
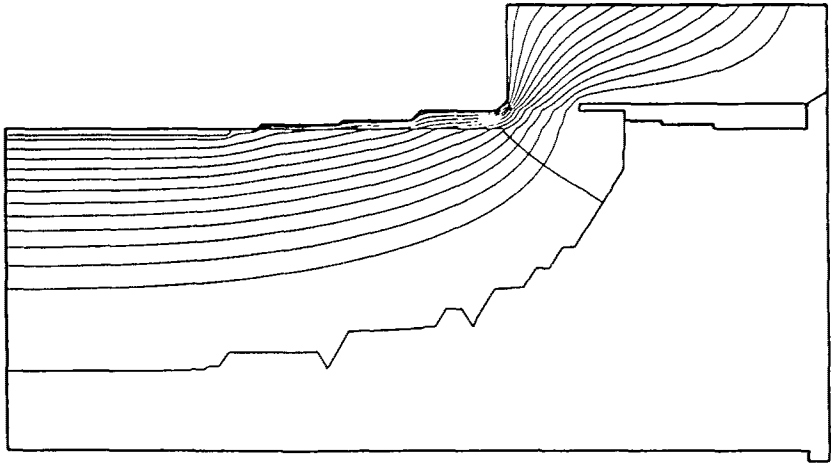

Figure 9: Level curves of final solution Ψ_6

References

[1] E. Falck and W. Gerlach, "Berechnung der Durchbruchsspannung von planaren pn-Übergaengen mit mehrstufigen Feldplatten," *AEÜ*, vol. 43, pp. 328–334, 1989.

[2] A. Chynoweth, "Ionization rates for electrons and holes in silicon," *Phys. Rev.*, vol. 109, pp. 1537–1540, 1958.

[3] E. Falck, W. Feiler, and W. Gerlach. private communication.

[4] S. Selberherr, *Semiconductor Equations*. New York, Berlin, Heidelberg, Tokyo: Springer, 1984.

[5] P. Markowich, C. Ringhofer, and C. Schmeiser, *Semiconductor Equations*. New York, Berlin, Heidelberg, Tokyo: Springer, 1990.

[6] C. Hunt and N. Nassif, "On a variational inequality and its application in the theory of semiconductors," *SIAM J. Num. Anal.*, vol. 12, pp. 938–950, 1975.

[7] R. Bank, *PLTMG: A Software Package for Solving Elliptic Partial Differential Equations. User's Guide 6.0.* Frontiers in Applied Mathematics 7, SIAM, 1991.

[8] P. Deuflhard, P. Leinen, and H. Yserentant, "Concepts of an adaptive hierarchical finite element code," *IMPACT*, vol. 1, pp. 3–35, 1989.

[9] R. Roitzsch and R. Kornhuber, "BOXES – a program to generate triangulations from a rectangular domain description," Technical Report TR90–9, Konrad-Zuse-Zentrum (ZIB), 1990.

[10] R. Kornhuber and R. Roitzsch, "Self adaptive finite element simulation of reverse biased pn-junctions." Submitted to Int. J. Numer. Meth. Eng., 1991.

[11] M. Adler, V. Temple, and R. Rustay, "Theoretical basis for field calculations on multi-dimensional reverse biased semiconductor devices," *Solid-State Electron*, vol. 25, pp. 1179–1186, 1982.

[12] R. Glowinski, *Numerical Methods for Nonlinear Variational Problems*. New York, Berlin, Heidelberg, Tokyo: Springer, 1984.

[13] R. Hoppe and R. Kornhuber, "Multilevel preconditioned cg-iterations for variational inequalities," in *Preliminary Proceedings of the 5th Copper Mountain Conference on Multigrid Methods* (S. M. et al., ed.), (Copper Mountain, Colorado), 1991.

[14] I. Babuška and W. Rheinboldt, "Error estimates for adaptive finite element computations," *SIAM J. Num. Anal.*, vol. 15, pp. 736–754, 1978.